

Boundary Layer Protuberance Simulations in Channel Nozzle Arc-Jet

J.J. Marichalar¹, M.E. Larin²
Jacobs Technology, Houston, TX 77058, USA

C.H. Campbell³
NASA Johnson Space Center, Houston, TX 77058, USA

and

M.V. Pulsonetti⁴
NASA Langley Research Center, Hampton, VA 23681, USA

Two protuberance designs were modeled in the channel nozzle of the NASA Johnson Space Center Atmospheric Reentry Materials and Structures Facility with the Data-Parallel Line Relaxation computational fluid dynamics code. The heating on the protuberance was compared to nominal baseline heating at a single fixed arc-jet condition in order to obtain heating augmentation factors for flight traceability in the Boundary Layer Transition Flight Experiment on Space Shuttle Orbiter flights STS-119 and STS-128. The arc-jet simulations were performed in conjunction with the actual ground tests performed on the protuberances. The arc-jet simulations included non-uniform inflow conditions based on the current best practices methodology and used variable enthalpy and constant mass flow rate across the throat. Channel walls were modeled as fully catalytic isothermal surfaces, while the test section (consisting of Reaction Cured Glass tiles) was modeled as a partially catalytic radiative equilibrium wall. The results of the protuberance and baseline simulations were compared to the applicable ground test results, and the effects of the protuberance shock on the opposite channel wall were investigated.

Nomenclature

h_f	=	heating rate augmentation factor
h_{tot}	=	total enthalpy, Btu/lbm
k	=	protuberance height
q	=	heating rate, Btu/ft ² -sec
\dot{m}	=	mass flow rate, lbm/s
T_{pro}	=	surface temperature from protuberance thermocouple location (in °R)
T_{ref}	=	surface temperature from reference thermocouple location (in °R)

I. Introduction

THE Boundary Layer Transition Flight Experiment (BLTFE) flown on STS-119 and STS-128 was designed to investigate turbulent boundary layer transition heating effects caused by protuberances on the windward thermal protection system (TPS) of the U.S. Space Shuttle Orbiter. The BLTFE was designed to specifically measure heating on the protuberance and directly downstream of the protuberance where turbulent transition heating was likely to occur. The study of early boundary layer transition due to protuberances was initiated after the appearance of

¹ Aerothermal Engineer, Aerothermal and Flight Dynamics, 2224 Bay Area Blvd, Houston, TX 77058/Mail Stop JE-B3-2, Member AIAA.

² Aerothermal Engineer, Aerothermal and Flight Dynamics, 2224 Bay Area Blvd, Houston, TX 77058/Mail Stop JE-B3-2.

³ Aerothermal Engineer, Applied Aerosciences and CFD Branch, 2101 NASA Pkwy., Houston, TX 77058/Mail Stop EG3, Senior Member AIAA.

⁴ Senior Research Scientist, Aerothermodynamics Branch, Hampton, VA 23681/Mail Stop AB.

protruding gap fillers from between the high-temperature reusable surface insulation (HRSI) tiles on the windward TPS of the Orbiter during previous missions^{1,2}.

In order to conduct the BLTFE, the principle investigators had to show flight mission managers that the additional heating due to the inclusion of a mounted protuberance on the windward side of the Orbiter would not cause the TPS to exceed its allowable temperature and cause significant damage to the vehicle. The NASA Johnson Space Center (JSC) Atmospheric Reentry Materials and Structures Facility (ARMSEF), commonly known as the JSC 10 MW Arc-Jet Facility³, was used to test various protuberance configurations in the 24 in. x 24 in. test section of Test Position 1 (TP1) – the channel nozzle test configuration – in order to show that the protuberance and surrounding HRSI tiles would survive re-entry^{1,2}.

To help predict the extent of heating that could be expected on the protuberance during the arc-jet tests, computational fluid dynamics (CFD) simulations of the TP1 channel nozzle were performed at a single arc-jet test condition (fixed mass flow rate and bulk enthalpy) for the baseline calibration test and the tested protuberance configurations. The results of these ground test CFD simulations and how they compare to arc-jet test data are the subject of this paper.

II. Purpose and Objectives

The arc-jet CFD simulations were performed primarily in support of the BLTFE, but also served to enhance understanding of the NASA JSC arc-jet facility. The main objective for the study was to obtain heating rate augmentation factors, h_f , based on protuberance and baseline arc-jet CFD solutions. The heating rate augmentation factors along with surface temperatures from the arc-jet CFD solutions provide traceability to the flight environment and validation of CFD predictions and modeling methodologies with test data. A secondary objective was to examine the increased heating to the opposite channel wall due to the reflection of the shock wave from the protuberance.

III. Methodology and Assumptions

The following section outlines the methodology and assumptions used in the arc-jet CFD study for the BLTFE. The arc-jet test conditions and the use of non-uniform inflow conditions are discussed as well as the protuberance designs and the CFD code used to perform the analysis.

A. Arc-Jet Test Configuration

The arc-jet test data used in this study comes from two different test programs: calibration tests run in 2004 in support of Return-To-Flight (RTF) activities⁴ and recent BLTFE protuberance arc-jet tests³. The arc-jet tests applicable to this study were performed in the 24 in. x 24 in. test section of the NASA JSC arc-jet TP1 channel nozzle.

A variable configuration tile array made of Lockheed Insulation (LI) -900 HRSI tiles instrumented with thermocouples was used in the calibration tests and in the BLTFE tests as the carrier for the protrusion inserts. The protuberance tiles were 6 in. x 6 in. tiles fabricated with a fin-shaped protrusion of a specific height, k , and made of Boeing Rigid Insulation (BRI) -18. The entire tile array and protrusion were coated with partially catalytic reaction cured glass (RCG). A pre-test photograph of the variable configuration tile array for the BLTFE arc-jet test with the 0.35 in. protuberance tile insert installed is shown in Figure 1³.

The arc-jet tests were run with temperature-time profiles designed to target specific tile surface temperatures including 1700 °F and 2000 °F. The arc-jet CFD simulations were performed for the 1700 °F temperature condition and specific arc-jet test parameters: mass flow rate, $\dot{m} = 0.251$ lbm/s and bulk enthalpy, $h_{tot} = 5952$ Btu/lbm.



Figure 1. Pre-test photograph of the variable configuration tile array with protrusion tile insert ($k = 0.35$ in.)

B. Non-Uniform Inflow Conditions

The current best practices procedure requires that arc-jet channel nozzle CFD simulations be performed with non-uniform inflow conditions at the throat. The best practices procedure was developed by performing a parametric study varying CFD input boundary conditions for the baseline arc-jet channel nozzle simulations.

Non-uniform inflow conditions for the 1700 °F test condition were computed with the Nozzle Throat Conditions 3D code written by D. Saunders at NASA Ames Research Center. The code was used to create a 2D inflow profile at the channel nozzle throat by varying enthalpy and mass flow rate from the centerline to the nozzle wall based on a sinusoidal function. Although the mass flow rate is allowed to be varied, the best practices procedure requires it to be constant across the nozzle throat. The ratio of centerline enthalpy to bulk enthalpy for the non-uniform inflow conditions is 2.09, according to the best practices procedure.

C. DPLR CFD Code

The Data Parallel Line Relaxation (DPLR) CFD code⁵ was used to perform all of the arc-jet CFD simulations. DPLR is a Reynolds-Averaged Navier-Stokes code and has been used extensively in modeling high-temperature reacting-gas flows. The code was run locally on an SGI Altix cluster at NASA JSC. Laminar solutions were assumed for all simulations. Best practices guidelines were used to determine when steady-state convergence had been achieved for each solution.

D. Baseline CFD Simulations

The baseline arc-jet CFD simulations were run for a quarter of the channel nozzle geometry, reducing solution computational time by taking advantage of the two planes of symmetry. Except for the test section wall, which was modeled as a radiative equilibrium wall with a RCG catalytic coating, all walls were modeled as fully catalytic isothermal walls with a cold-wall temperature of 80 °F. Instead of only modeling the 24 in. x 24 in. test section as RCG, the entire wall was modeled as RCG to simplify the complexity of the simulation.

The use of symmetry planes induces a restrictive modeling assumption: both the test section wall and the opposite channel wall are modeled as radiative equilibrium walls with RCG catalytic coatings. In order to compute accurate opposite wall heating augmentation factors, a second truncated simulation (without symmetry planes) was performed for the test section only with a radiative equilibrium test wall and fully catalytic isothermal side walls and opposite wall.

E. Protuberance CFD Simulations

A total of five protuberance geometries were used in the arc-jet CFD simulations. However, only the two final protuberance designs, which were tested in the arc-jet and flown on STS-119 and STS-128, are discussed in this study. The final versions of the protuberance designs – with heights of 0.25 in. and 0.35 in. – were run with non-uniform inflow conditions and were both fin-shaped. The 0.25 in. protuberance geometry is shown in Figure 2a along with the surface grid used for the simulation. The 0.35 in. protuberance geometry is a similar design and uses a similar surface grid as shown in Figure 2b.

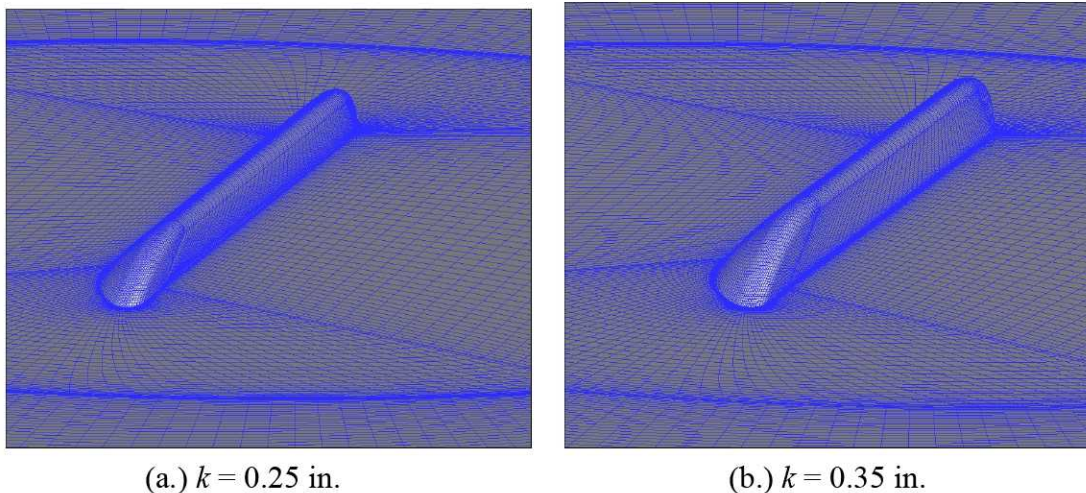


Figure 2. Protuberance grid.

F. Heating Augmentation Factors

The heating rate augmentation factors from the arc-jet CFD solutions and arc-jet test data were compared to understand how well CFD predictions and ground tests model the flight environment. The heating augmentation factors, h_f , for the arc-jet CFD solutions were computed with a method developed specifically for the arc-jet tests³. A ratio of radiative equilibrium heating rates is computed as in Eq. (1) below:

$$h_f = \left(\frac{T_{pro}}{T_{ref}} \right)^4 \quad (1)$$

The surface temperatures are extracted from the CFD solutions at the thermocouple (TC) position on the protuberance and at an upstream reference location that is undisturbed by the inclusion of the protuberance.

IV. Results

The following section discusses the results of the present study. The baseline and protuberance solutions are examined along with the derived heating augmentation factors. In addition, the results of the CFD simulations are compared to the arc-jet test data from the calibration and protuberance test runs.

A. Baseline Solutions

As noted before, multiple baseline solutions were computed for the fixed arc-jet condition corresponding to a reference surface temperature of 1700 °F. A full channel nozzle solution was computed for a quarter grid simulation with the best practices non-uniform inflow conditions. Truncated solutions, modeling all four walls of the 24 in. x 24 in. test section only, were also computed. The truncated solutions were needed in order to accurately derive opposite wall heating augmentation factors and also served to verify the inflow boundary conditions passed to the truncated solutions from the full channel nozzle solution.

Figure 3 shows the heating rate for the full channel nozzle (quarter grid) solution. The heating rate drops rapidly as the nozzle expands from the 2 in. x 2 in. throat. There is also a noticeable drop in heating rate as the flow transitions from the fully catalytic isothermal wall to the RCG wall. The heating to the 2 in. side wall drops more rapidly than the heating to the main (expanding) wall.

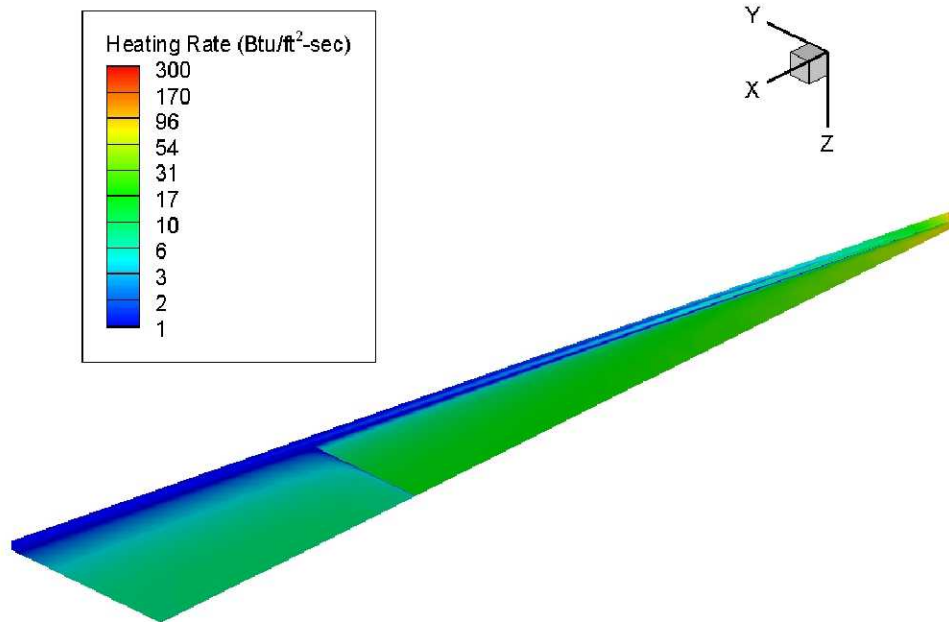


Figure 3. Full nominal solution (quarter grid).

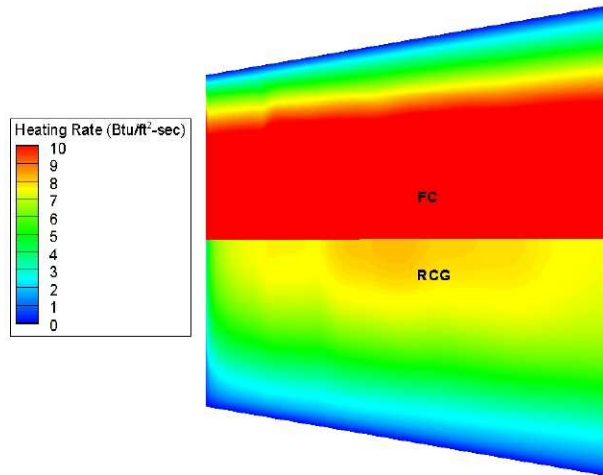


Figure 4. Truncated nominal solution (four wall grid) showing RCG wall and fully catalytic cold wall.

Figure 4 compares the RCG wall and fully catalytic (FC) cold wall for the truncated four-wall solution. Heating rates on the fully catalytic isothermal wall are approximately twice as large as heating rates on the RCG wall.

The flow field from the baseline solutions was used as input to the truncated protuberance simulations, which modeled only the 24 in. x 24 in. test section of the TP1 channel nozzle.

B. Protuberance Solutions and Opposite Wall Effects

The final protuberance designs that were tested in the arc-jet ground tests and flown on the Orbiter were fin-shaped with protuberance heights of 0.25 in. and 0.35 in. The solutions for both the 0.25 in. and 0.35 in. protuberances were truncated to cut down on solution time and make use of the baseline solutions.

Figures 5a and 5b show the heating rates to the surface of the 0.25 in. protuberance and the opposite wall, respectively. There is evidence of a complex reflected shock wave pattern on the opposite wall and increased heating downstream of the protuberance due to re-circulating flow. Although the simulation was run for laminar flow, the results suggest the flow may be transitional or turbulent downstream of the protuberance. Some skewing in the grid patchwork is evident on the opposite wall and causes a discontinuity in the solution near the zonal boundaries. This discontinuity effect is apparent in both of the opposite wall solutions but has little effect on the final results.

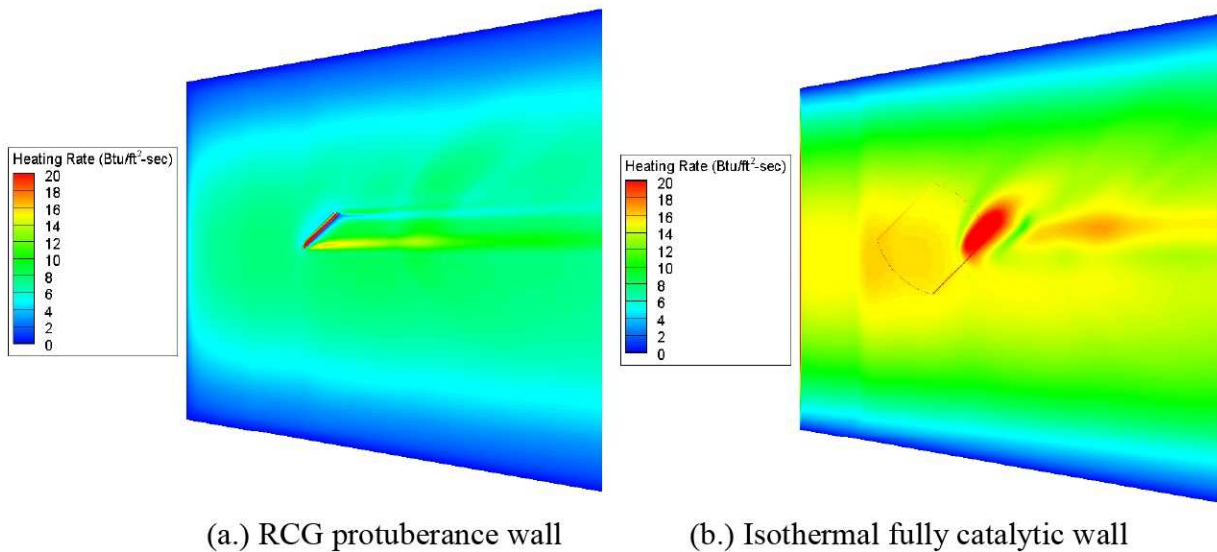


Figure 5. Heating rates on the surface of the 0.25 in. protuberance and the opposite wall.

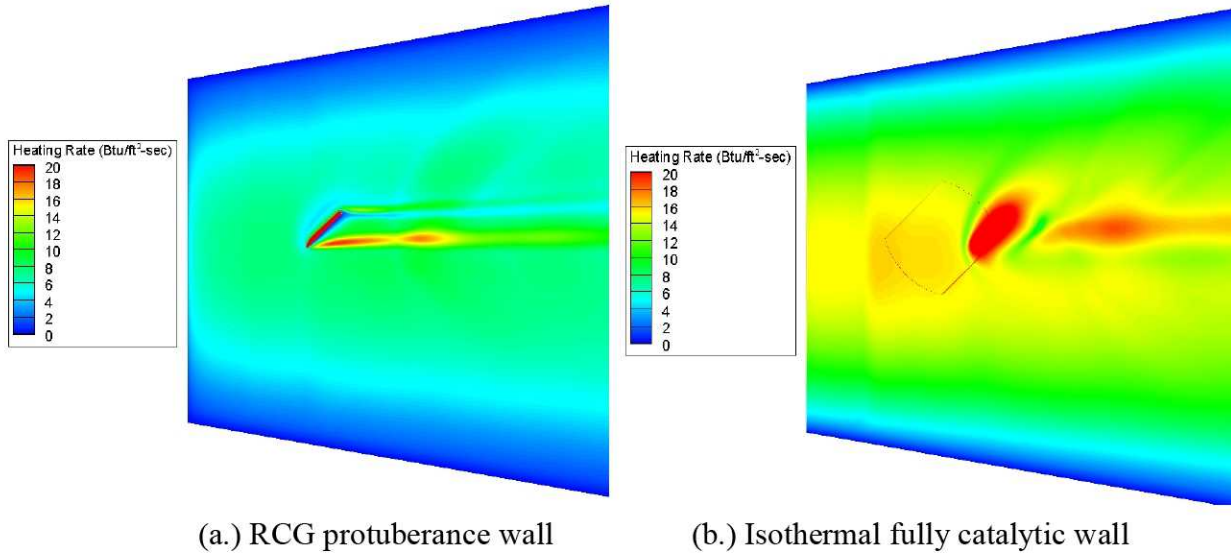


Figure 6. Heating rates on the surface of the 0.35 in. protuberance and the opposite wall.

Figures 6a and 6b show the heating rates to the surface of the 0.35 in. protuberance and the opposite wall, respectively. Compared to Figure 5, the 0.35 in. protuberance solution shows that heating is slightly more severe on the protuberance, the downstream tiles and the opposite wall. The flow structure for the 0.35 in. protuberance solution appears to be very similar to that of the 0.25 in. protuberance solution and suggests the flow downstream of the protuberance may be transitional or turbulent.

C. Heating Rate Augmentation Factors

Based on the protuberance and baseline solutions described above, the heating rate augmentation factors were computed with Eq. (1). Surface temperatures were extracted from the CFD solutions at the specific thermocouple locations from the arc-jet test.

Figures 7a and 7b display the thermocouple measurements and locations along with surface temperatures on and around the protuberances. The thermocouple measurements included in Figure 7 are from the arc-jet test runs which most closely matched the targeted reference condition. Figure 7a shows that there is good agreement between the CFD solution and the arc-jet test data at all of the thermocouple locations. The temperatures differ the most at the

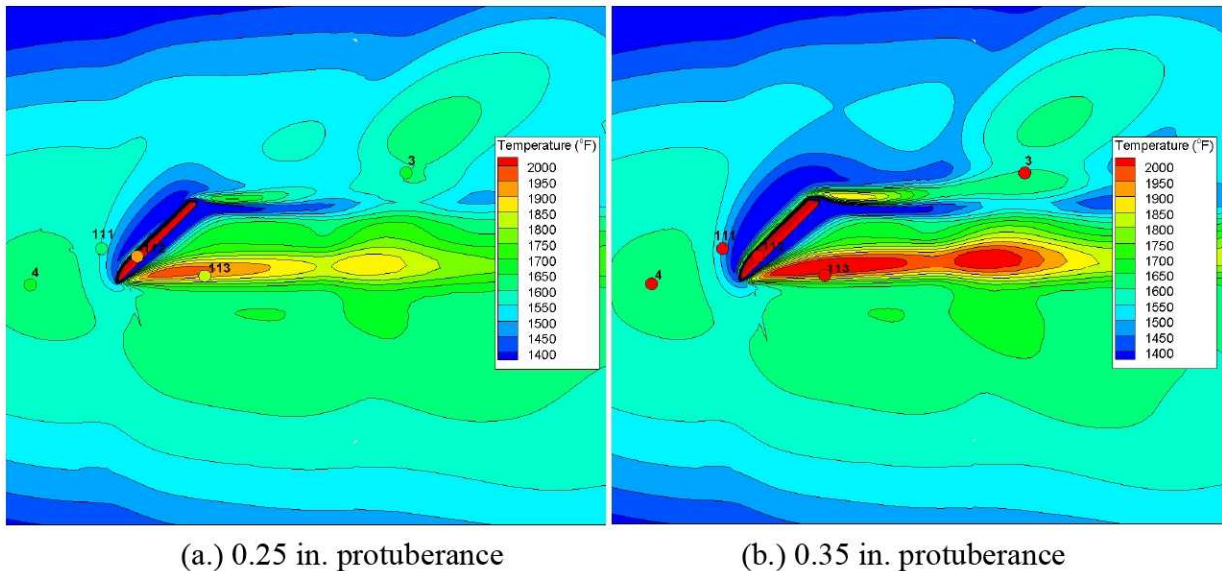


Figure 7. CFD surface temperatures compared with thermocouple measurements for protuberance tests.

thermocouples on the tip of the protrusion and immediately downstream of the protrusion. Figure 7b reveals that the arc-jet test thermocouple measurements are much higher than the CFD solution at all locations except on the tip of the protrusion. The large temperature differences are likely due to the mismatch of the targeted reference condition for the arc-jet test run and the CFD simulation, but could also be caused by the higher reflected heat flux from the polishing of the opposite wall that occurred prior to the 0.35 in. protuberance test run³.

Table 1. Surface temperatures extracted from protuberance solutions at thermocouple locations.

TC#	location	Distance from Throat (in.)	Distance from Centerline (in.)	CFD	CFD
				Temperature ($k = 0.25$) ($^{\circ}\text{F}$)	Temperature ($k = 0.35$) ($^{\circ}\text{F}$)
4	array upstream	73.938	0.000	1607	1607
3	array downstream	86.915	3.907	1589	1579
111	insert upstream	76.402	1.264	1542	1490
112	protrusion	77.634	0.990	2246	2488
113	insert downstream	79.960	0.306	1931	1947

The surface temperatures extracted from the protuberance solutions at the thermocouple locations shown in Figure 7 are listed in Table 1 along with the location of the thermocouple. TC #4 and TC #112 correspond to the reference thermocouple and the protuberance thermocouple, respectively, used to compute the heating rate augmentation factors. Based on the drop in temperature measured at TC #111, it appears that the 0.35 in. protuberance causes a larger upstream disturbance than the 0.25 in. protuberance.

Based on Equation (1), heating rate augmentation factors were computed for the two CFD protuberance simulations and all of the protrusion arc-jet tests. The computed heating rate augmentation factors are listed in Table 2 along with the input temperatures and the corresponding protuberance height. The average augmentation factor for the 0.25 in. and 0.35 in. protuberance arc-jet tests are 1.52 and 2.13, respectively.

Table 2. Heating rate augmentation factors computed from CFD simulations and arc-jet test runs.

	k (in.)	T_{ref} ($^{\circ}\text{F}$)	T_{pro} ($^{\circ}\text{F}$)	h_f
CFD	0.25	1607	2246	2.94
CFD	0.35	1607	2488	4.14
Test	0.25	1530	1740	1.5
Test	0.25	1590	1790	1.4
Test	0.25	1670	1910	1.5
Test	0.25	1800	2110	1.7
Test	0.25	2000	2260	1.5
Test	0.35	2070	2590	2.1
Test	0.35	2230	2730	2
Test	0.35	2250	2890	2.3

The listed reference temperatures reveal that the arc-jet test runs for the 0.35 in. protuberance did not match the 1700 $^{\circ}\text{F}$ reference temperature used for the CFD simulation. However, qualitatively, the results reveal that the CFD simulations predict heating rate augmentation factors approximately twice as large as the arc-jet test data.

D. Comparisons with Arc-Jet Test Data

The arc-jet test data used in this study comes from two different test programs. Calibration tests run in 2004 in support of RTF activities⁴ and recent BLTFE protuberance arc-jet tests³ produced surface temperature data obtained from thermocouple measurements at specific locations on the RCG-coated HRSI variable configuration tile array. As mentioned in the methodology and assumptions, the CFD simulations were all run for a specific arc-jet condition ($\dot{m} = 0.251$ lbm/s and bulk enthalpy, $h_{tot} = 5952$ Btu/lbm) corresponding to a target reference temperature of 1700 $^{\circ}\text{F}$. This specific arc-jet condition was based on the calibration test run performed in 2004, and therefore, the baseline solution would offer the best one-to-one comparison to the arc-jet test data. Although the protuberance arc-

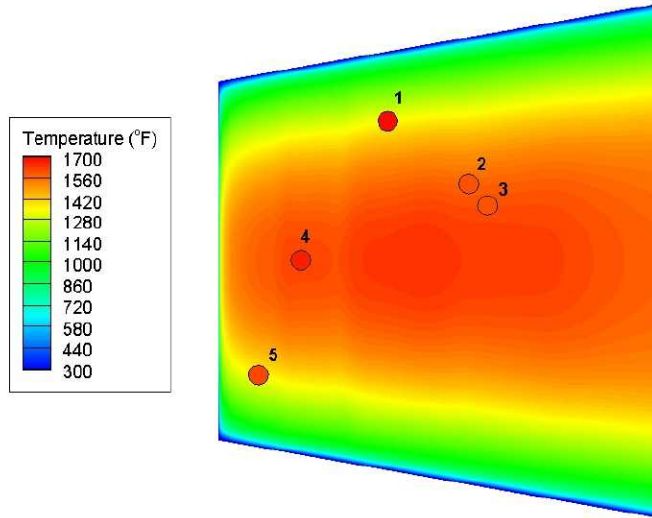


Figure 8. CFD surface temperatures compared with thermocouple measurements for calibration test.

jet test runs and CFD simulations set out to match the 1700 °F reference temperature, it is evident from the reference temperatures listed in Table 2 that an exact match was not achieved.

A comparison of the RCG wall surface temperatures and the arc-jet test thermocouple data is shown in Figure 8 to highlight the differences between the CFD baseline simulations and the ground test data. The surface temperatures from the CFD solution match well with the test data along the centerline, but differ more at the off-centerline thermocouples.

Table 3 lists the surface temperatures extracted from the CFD solutions and the arc-jet thermocouple measurements along with the thermocouple locations. The surface temperatures from the CFD solution match within ± 40 °F with the test data along the centerline, but are approximately 350 °F lower than the test data at the furthest off-centerline thermocouples.

Table 3. Surface temperatures extracted from baseline solution at thermocouple locations compared to arc jet test data.

TC#	Distance from Throat (in.)	Distance from Centerline (in.)	Arc Jet Temperature (°F)	CFD Temperature (°F)
1	80.267	-10.133	1696	1365
2	86.133	-5.600	1601	1603
3	87.467	-4.000	1593	1633
4	74.000	0.000	1669	1636
5	70.933	8.267	1608	1352

V. Concluding Remarks

Two protuberance designs ($k = 0.25$ in. and 0.35 in.) were modeled in the channel nozzle of the NASA JSC 10 MW Arc-Jet Facility with the DPLR CFD code. The arc-jet simulations were performed in conjunction with the actual ground tests performed on the protuberances. The heating on the protuberance was compared to nominal baseline heating at a single fixed arc-jet condition in order to obtain heating rate augmentation factors which have been used in the traceability study between ground test and flight. The results of the protuberance and baseline simulations were compared to the applicable ground test results, and the effects of the protuberance shock on the opposite channel wall were investigated.

The protuberance arc-jet simulations included non-uniform inflow conditions based on the current best practices methodology and used variable enthalpy and constant mass flow rate across the throat. Channel walls were modeled

as fully catalytic isothermal surfaces, while the RCG test section was modeled as a partially catalytic radiative equilibrium wall. The best practices methodologies employed in this study were adequate enough to achieve good agreement with test data along the centerline of the calibration test run. However, improvements will be needed in order to rectify the surface temperature differences for the off-centerline measurement locations.

Surface temperatures extracted from protuberance CFD simulations were compared to arc-jet test thermocouple measurements and indicated good agreement for the 0.25 in. protuberance. The large temperature differences observed for the 0.35 in. protuberance were likely due to a mismatch of the targeted reference condition for the arc-jet test run and the CFD simulation, but could also have been caused by the higher reflected heat flux from the polishing of the opposite wall that occurred prior to the 0.35 in. protuberance test run³.

Opposite wall heating from the reflected protuberance shockwave was substantial for both protuberance simulations. However, because heating in the upstream portion of the TP1 channel nozzle is equal to or more severe than the heating observed on the opposite wall of the 24 in. x 24 in. test section, it was determined by the principle investigators and the arc-jet facility personnel that the level of heating on the opposite wall was not high enough to cause any damage to the facility. The opposite wall was examined after the protuberance testing according to the standard operating procedure for the facility and no damage was noticed.

Future work for the BLTFE will include more protuberance CFD solutions for different protuberance heights along with additional ground and flight tests. Non-uniform inflow conditions and best practice applications will also be revised to more closely match arc-jet calibration test data.

References

¹Anderson, B. P., "BLT Flight Experiment Overview and In- Situ Measurements," Paper AIAA-2010-0240 Presented at the 48th AIAA Aerospace Sciences Meeting in Orlando, FL, January 4-7, 2010.

²Campbell, C. H., Garske, M. T., Kinder, G. R., Berry, S. A., "Orbiter Entry Boundary Layer Flight Testing" Paper AIAA-2008-635 Presented at the 46th AIAA Aerospace Sciences Meeting and Exhibit in Reno, NV, January 7-10, 2008.

³Larin, M. E., Bulot, E. M., Schoolmeyer, W. H., "Boundary Layer Transition Trip HRSI TPS Tests at NASA JSC Arc-Jet Facility," Technical Report JSC-64650/ESCG-4380-09-AFD-DOC-0009, Jacobs Technology/ESCG, Houston, Texas, September 2009.

⁴Larin, M. E., Marichalar, J. J., Fredo, J. A., Rochelle, W. C., Campbell, C. H., "Results of Calibration Tests in Channel Nozzle of JSC Arc-Jet Facility," Technical Report JSC-62673/LMSEAT-34416, Lockheed Martin Space Operations, Houston, Texas, August 2004.

⁵Wright, M. J., Candler, G. V. and Bose, D., "Data-Parallel Line Relaxation Method for Navier-Stokes Equations," AIAA Journal, Vol. 36, No. 9, Sept. 1998.